

Development of the components of an atmospheric dispersion

FINAL REPORT

PI

István Lagzi

Department of Physics

Budapest University of Technology and Economics



M Ú E G Y E T E M 1 7 8 2

2020

Short summary of the project: The development of atmospheric dispersion models requires complex thinking and interaction of researchers from different fields. For simulating the dispersion of air pollutants, various modelling approaches have been developed. Simulations with these models must have a high degree of accuracy and must be achieved faster than real time to be of use in an effective decision support. Therefore, accurate and fast simulation of the dispersion of toxic chemical substances or radionuclides in the atmosphere is one of the most important and challenging tasks in atmospheric sciences. The primary aim of this project was the development of the components of a multi-scale atmospheric dispersion modelling system and an air quality prediction system that allow the investigation of pollution load as a result of accidental and continuous emissions into the atmosphere. We verified different types of dispersion models based on the measurements and also a wide range inter-comparison of each model. Based on the experiences of preliminary model simulations we proposed new model parameterizations. We realized the developments and applications of different types of dispersion models operating from local to continental scales. Another main part of our research was the application of a linear multi-model fusion method for urban air quality prediction in Hungarian air pollution research.

Research in a nutshell

- (i) We developed a new atmospheric dispersion model (RAPTOR) to simulate the dispersion of Fukushima-derived radionuclides and their homogenization in the atmosphere. The results were published in *Scientific Reports*.¹
- (ii) We coupled and used the WRF-Chem model to predict the air quality of Budapest. The results of this investigation were published in *Időjárás*.²
- (iii) We simulated the atmospheric dispersion of radionuclides by different models. The results were published in *PLOS One*.³
- (iv) We applied a linear multi-model fusion method to downscale of PM_{2.5} predictions from CAMS air quality models to urban monitoring sites in Budapest. The work was published in *Atmosphere*.⁴
- (v) We wrote an invited review article on numerical models predicting the atmospheric dispersion of radionuclides published in the *Journal of Environmental Radioactivity*.⁵
- (vi) We calculated the traffic originated urban air pollution load by using an atmospheric-chemistry model. We intend to publish these results soon.
- (vii) We develop a model to simulate the air pollution levels in the atmosphere using dissipative particle dynamics (DPD). We are planning to publish these results as well.

1. Predictability of the dispersion of Fukushima-derived radionuclides and their homogenization in the atmosphere

The Fukushima Daiichi nuclear disaster has been the second most serious crisis of a nuclear power plant in the human history. The release period lasted over two months emitting a significant amount of radioiodine, radioxenon and radiocaesium as well as other isotopes such as plutonium. Besides the local to regional scale impacts of soil and water pollution, isotopes released into the atmosphere could be measured globally. Total atmospheric release was estimated to be 14000–15300 PBq of radioxenon and 340–800 PBq of other isotopes. The radioactive plume in the atmosphere moved towards the Pacific, reached North America in five days and Europe in eight days, and returned over Japan around the Northern Hemisphere within only 20 days. Although health concerns have not arisen out of Japan, Fukushima-derived radioiodine and radiocaesium could be identified in the entire Northern Hemisphere as a tracer of atmospheric dispersion. Measurements were made at several sites by international and national monitoring networks as well as research groups and expedition campaigns. The large number of data points allows the identification of transport pathways as well as the evaluation of dispersion model performance and emission scenarios.

While monitoring stations provided valuable data for concentrations in the atmosphere, the emission term and its temporal variability was not known during the accident. The emission was caused by several different processes, including two hydrogen explosions, controlled release and uncontrolled emission for several weeks. Initial estimates of total ^{131}I release into the atmosphere ranged from 150 to 500 PBq. Modelling efforts focused on inverse methods that provided more accurate estimates of 65–400 PBq for total ^{131}I . Among others, the WSPEEDI (Worldwide System for Prediction of Environmental Emergency Dose Information) model has been used with data obtained from the Japanese measurement network to estimate a more detailed emission inventory and emission rates, resulting in a total ^{131}I emission of 124 PBq and ^{137}Cs emission of 8.8 PBq. Recently, the improved WSPEEDI-II model has provided an updated emission data and a detailed reconstruction of the events leading to the accidental release. This latest work concluded a total of 150 PBq ^{131}I and 14.4 PBq ^{137}Cs emission. Besides the increased total emission compared to the previous estimation, the results of WSPEEDI-II yielded an improved timeline for the first hydrogen explosion and the emission peak on the night 14–15 March.

We performed a study using a Lagrangian model to evaluate the predictability of the transport of the radioactive plume across the globe comparing modelled concentration values and arrival times to the measured data. We also investigated the improvement of modelled results provided by the WSPEEDI-II emission data compared to earlier reported WSPEEDI emission data. Additionally, based on geographical locations and arrival times we could group the measurement sites into clusters corresponding to different atmospheric transport pathways.

Model

In this study, we used the RAPTOR dispersion model for the simulation of arrival times and ^{131}I activity concentrations in the atmosphere for a 35-day period. This continental/global scale trajectory model was developed at the Eötvös Loránd University and Budapest University of Technology and Economics, Hungary. Four million particles were emitted and their trajectories were calculated for the entire simulation time. Each particle represented a fraction of the total activity that decreased with radioactive decay and wet deposition over time. The model used longitude–latitude horizontal and z (absolute) vertical coordinates. Digital elevation data from the Global Land One-km Base Elevation Project was used to provide more accurate results of plumes traversing complex terrain. Particles were moved along air parcel trajectories determined by the sum of the grid-scale wind and the subgrid-scale stochastic turbulent velocity, solving the ordinary differential equation with a simple first-order forward scheme. The turbulent velocities were calculated using the Langevin equation with turbulent parameters obtained from Hanna's parameterization. Atmospheric stability was characterized with the Monin–Obukhov-length calculated directly from heat flux data provided by the meteorological model. Aerosol wet scavenging was parameterized with a simple first-order deposition scheme assuming the same size distribution for both iodine and caesium aerosols. Scavenging coefficients were calculated separately from large-scale and convective precipitation rates using empirical parameters

Results

Predictability of the arrival time of the plume was different among regions, and depended largely on the complexity of the atmospheric circulation systems governing the dispersion. The best correlations can be observed in the tropical and Arctic regions due to the relatively stable trade and polar winds. In American and European midlatitudes, the early detections were generally well predicted by the model, however, the later regional-scale mixing could not be captured, significantly underestimating the arrival times at several sites.

It should be noted that concentration patterns and model performance was studied for a limited number of measurement sites and therefore may not be representative for entire regions. The density of measurement network was fine in Europe, North America and Eastern-Southeastern Asia, however, much coarser in Pacific and Arctic regions. Therefore, measurements in the latter regions are less representative for the absolute peak concentration and predictability of the entire area.

In Asia, there is a contradiction in the question of westward moving plumes between 20 and 28 March. Reported measurements in South Korea and China suggest that the first detections were caused by the global hemispheric transport on 28–31 March. This arrival time of the high tropospheric plume is supported by our model, however, model results showed earlier surface detections in South Korea between 21 and 26 March and a slow mixing over China between 21 and 31 March due to westward transport from Fukushima (Figure 1.1). It has been shown in previous model simulations that an anticyclonic system forced the plume to northwestward direction between 20 and 24 March that could marginally reach

Northeastern China and the Korean Peninsula. Our model also suggests further westward dispersion to mainland China by 26 March. However, this early transport was not supported by other model and measurement results. Contrary to these, detection of Fukushima-derived radionuclides was reported from a study in Xi'an, Central-Eastern China on 23 March with a significant peak on 25 March, more according to our estimates. To assess this contradiction, we used results from the online version of HYSPLIT (Hybrid Single Particle Lagrangian Integrated Trajectory Model) applied for the Fukushima case using the Transfer Coefficient Matrix (TCM) method. The concentration timeline for Xi'an and Seoul provided by HYSPLIT radically supported the scenario of a significant westward transport with arrival times as early as 15–16 March in Xi'an and Seoul. HYSPLIT also showed the reported peak in Xi'an on 25 March. The high uncertainty of the pathway and surface detectability of early westward moving plumes from Fukushima points out the importance of further studies.

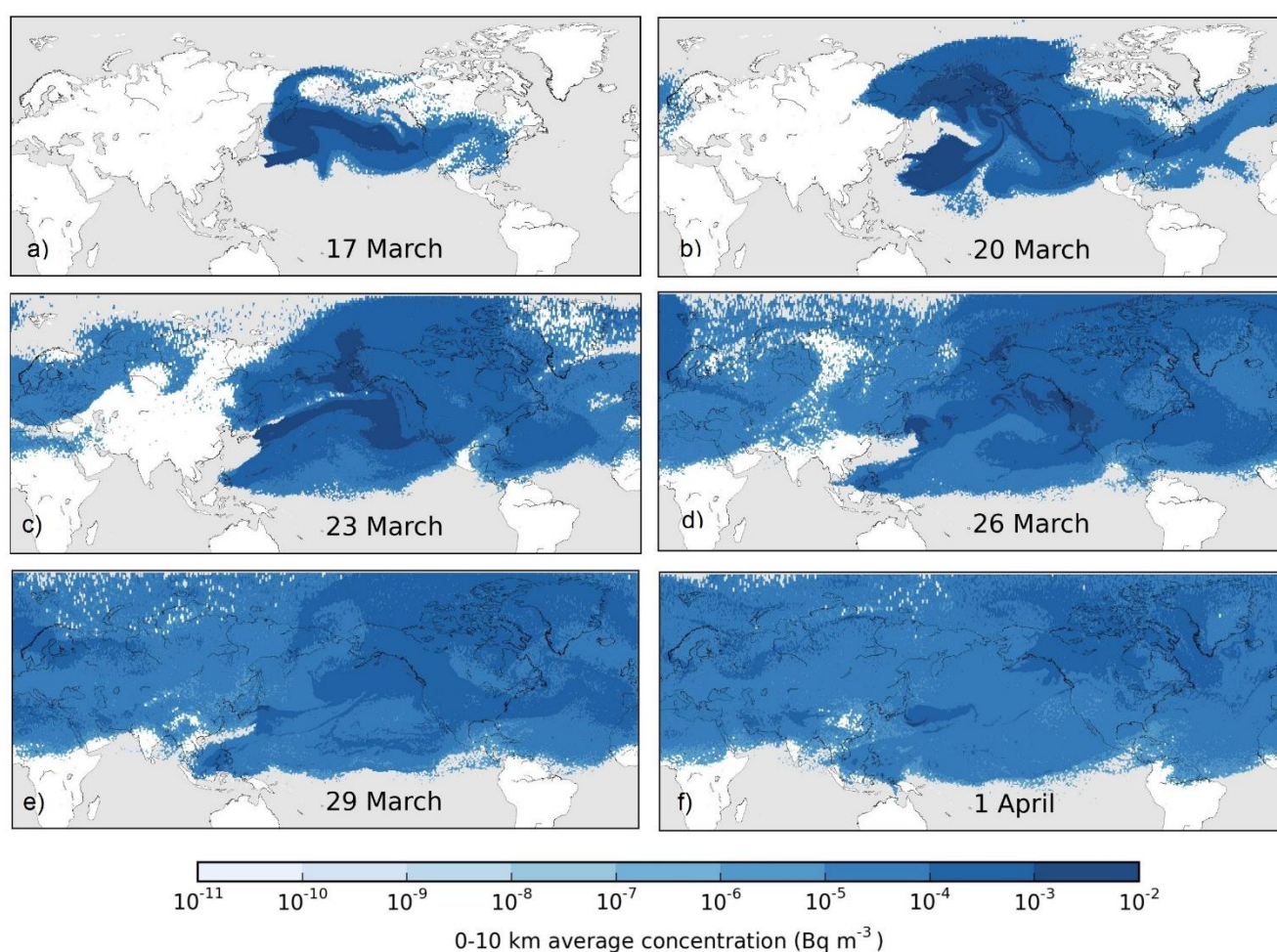


Figure 1.1 Modelled ^{131}I activity concentrations in the troposphere (0–10,000 m) on the 6th, 9th, 12th, 15th, 18th and 21st days after the initial release.

The initial ratio of gaseous to total ^{131}I was obtained from the emission scenario, however, this ratio was decreased by wet scavenging of aerosols throughout the dispersion. Wet scavenging of ^{131}I is one of the most uncertain processes of atmospheric dispersion that is highly dependent on the ratio of the chemical forms of iodine in the plume as well as precipitation and cloud data obtained from global

meteorological models. Despite neglecting all sink processes except radioactive decay and wet scavenging, our results showed an overall underprediction of ^{131}I peak concentrations, a similar phenomena that had been assessed in previous modelling studies.

Initial gaseous/total ratio was measured between 30 and 67% in Japan and 40 and 100% in Europe and North America. Wet scavenging was shown to decrease the contribution of particle form to the total, therefore largest gaseous/total ratios were measured at locations where transport was permanently accompanied with precipitation, mostly related to the jet stream. The development of WSPEEDI-II for the latest emission estimate focused largely on the representation of different deposition processes for gaseous and particulate iodine. They assumed 50% gaseous/total ratio for the initial, largest emissions and an integrated ratio of 54% for the entire release. Based on measurements in North America and Europe, an average atmospheric ratio of $76.7 \pm 12\%$ was calculated for the period until 22 April. This yields an average uncertainty of concentrations with a factor of 1.5 due to wet scavenging which is comparable to the uncertainty of the initial ratio of aerosol and gas forms. Atmospheric half-life of particulate ^{131}I was estimated to be 6 days (median) with a range between 3.25 and 8.5 days.

2. Online coupled modelling of weather and air quality of Budapest using the WRF-Chem model

Outdoor air pollution is a serious environmental issue in Hungary, especially in winters. Ambient air quality thresholds for NO₂ and PM₁₀ are regularly exceeded. The Aphekom project found that in the period of 2008–2011, the life expectancy was decreased by 19 months in Budapest due to the outdoor air pollution. The World Health Organization (WHO) found that in 2012, approximately 8,000 premature deaths could be attributed to polluted ambient air in Hungary. The main sources of PM₁₀ and ozone air pollution are domestic heating, road traffic and large-scale transport of air pollutants. The European Union expects effective strategies to diminish the effect of air pollution, however, policymaking requires the good understanding of the fine scale urban environmental processes and the reliable prediction of air quality for the following days. Operational air quality prediction is performed by the Hungarian Meteorological Service using the CHIMERE air dispersion model offline coupled with the WRF numerical weather prediction model.

Online coupled weather and air quality modelling have become a powerful and widely applied tool to predict and evaluate air pollution on the regional scale. In Europe, numerical air quality forecasts are available from several continental scale atmospheric chemistry transport models, mainly those of the Copernicus Atmospheric Monitoring Service (CAMS) cooperation (<https://atmosphere.copernicus.eu/>). Its models use a grid of 0.1 degree resolution on the continental scale to operationally predict atmospheric concentrations of the main air pollutants, as well as pollens and volcanic ash. However, for cities and other sensitive areas, a finer model resolution might be necessary, especially if the emission inventory is available on a fine scale. This can be achieved by a nested atmospheric chemistry transport model that can reach very fine (1–3 km) resolution for a limited area.

WRF-Chem is an atmospheric chemistry and transport module online integrated with the extremely popular Weather Research and Forecast (WRF) numerical weather prediction model. It solves the governing equations of atmospheric dynamics, tracer transport and chemical reactions within one model system, sharing the same grid and timesteps. Online coupling enables the model to simulate the feedbacks of air pollution on the weather, especially the effects of atmospheric aerosols. On the other hand, online coupling of the meteorology and transport simulation can gain better accuracy in complex weather situations by accessing the full planetary boundary layer (PBL) parameterization of the weather forecast model and avoiding the information bottleneck of derived output parameters.

WRF-Chem has been used in several countries for regional and urban scale air pollution forecast. In recent years, nested WRF-Chem simulations focusing on urban air pollution have been presented for cities such as Berlin, Madrid, Los Angeles, for several metropolitan regions in China and even for the complex terrain of Kathmandu. However, comparison studies proved that WRF-Chem model results show a large sensitivity on the selection of the chemistry scheme, both regarding the tropospheric ozone and secondary aerosol formation. For example, in a photochemical box model, 25% difference was found between NO_x concentrations obtained with different chemical mechanisms.

We investigated the applicability of WRF-Chem (numerical weather prediction and atmospheric chemistry and transport) model to simulate and estimate concentration levels and diurnal variation of ozone and nitrogen oxides in Budapest and other sites in Hungary (Figure 2.1).

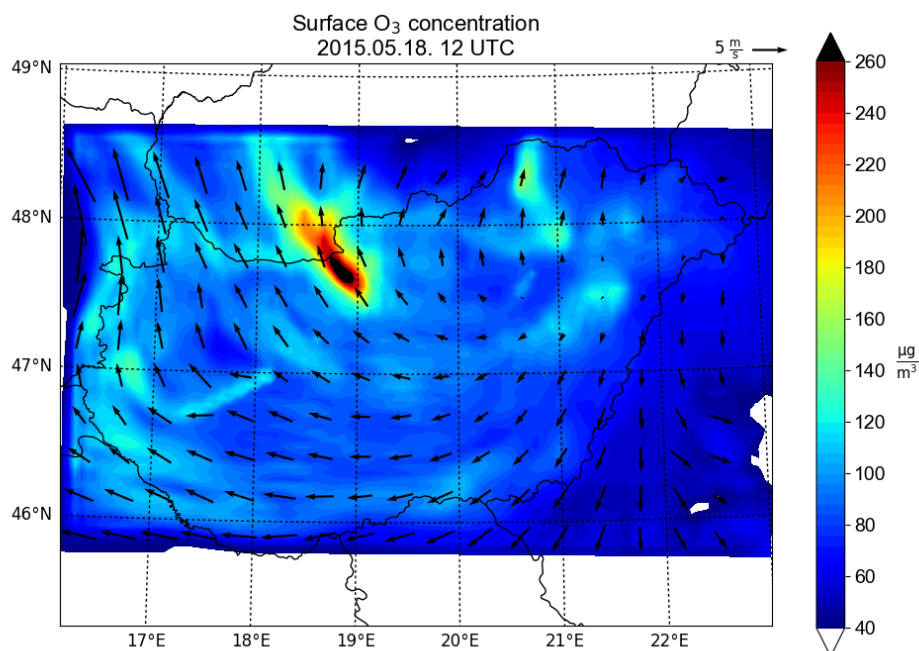


Figure 2.1 Simulated near-surface ozone concentration and 10 m wind field at 12 UTC, 18th May 2015, using WRF-Chem with the RADM2-KPP chemical mechanism

Results

All simulations were performed with the WRF-Chem model using two nested domains covering Central Europe and Hungary. With this method, a relatively low horizontal resolution (5 km) could be achieved at an acceptable computational cost. Provided with meteorological boundary conditions from the Global Forecast System (GFS) and emission data from the NERC–IIR national emission inventory, the model could simulate the atmospheric dispersion of pollutants and photochemical ozone formation.

Model capabilities were demonstrated through a case study for 17–18 May 2015, comparing two chemical mechanisms (RADM2 and CBMZ), both with and without the kinetic pre-processor (KPP). Emission inventories of NO_x, non-methane VOCs and CO were considered. Model results were compared to measurements taken at monitoring sites of the Hungarian Air Quality Network (OLM). The diurnal cycle of ozone was generally well captured by the model despite the stationary emission field. However, a large difference was found between the two applied chemical mechanisms. RADM2 provided generally higher and more realistic ozone concentrations, however, it seriously overestimated NO₂ levels. Results showed low sensitivity on the application of the kinetic pre-processor and the initial NO/NO₂ ratio.

3. Numerical simulations of atmospheric dispersion of iodine-131 by different models

Very low ^{131}I concentrations were observed in some European stations, mainly in Central Europe, in October and November, 2011. Stations located in the Czech Republic, Austria, Germany, Poland, Slovakia, Sweden, France, Hungary, Ukraine and Russia have measured and informed the Incident and Emergency Centre (IEC) on the detection of very low levels of ^{131}I in air samples collected over intervals of several days. Measured concentration values in some European countries just reached the limit of detection and were not any health concern to the population. However, only a few months after the accident in Fukushima Dai-ichi Nuclear Power Plant in March 2011, these extremely low concentrations received more attention both from the public and the scientific communities. Although the measured concentrations were below the exposure limit, the International Atomic Energy Agency (IAEA) has initiated an investigation in order to find out the source of the elevated iodine concentrations. Backward trajectory simulations narrowed the possible locations of the source to Central Europe, however, they could not perform more accurate localization because of the long sampling period of measurement sites. The investigation led to result on 17 November 2011, when the Hungarian Atomic Energy Authority reported that during the period between January and May, and also between September and November, 2011, probably due to the improper operation of the filtration system, some ^{131}I , slightly higher than usual, had been released into the atmosphere from the laboratory of the Institute of Isotopes Ltd., Budapest. The Institute of Isotopes is dealing with the research, development and production of a wide variety of radioactive isotopes and other products for a broad range of application areas, especially healthcare, research and industry.

In this study, the dispersion of the radioactive plume and the spatial distribution of ^{131}I were simulated by different dispersion models over Central Europe. The applied models were the following:

- the HYSPLIT Lagrangian dispersion model of the National Oceanic and Atmospheric Administration (NOAA),
- the RAPTOR Lagrangian dispersion model, developed by the authors of the project,
- and the WRF-Chem Eulerian integrated atmospheric chemistry transport model.

Results

Atmospheric dispersion simulations have been carried out in cases of four 6-hour long ^{131}I release from Budapest in October and November 2011 (Figure 3.1). Model results from the Lagrangian dispersion model RAPTOR, developed in the framework of this project, were compared to those of Lagrangian HYSPLIT and Eulerian WRF-Chem, two of the most widely applied atmospheric transport models. Simulation results were evaluated based on reported detections in Dubna (Russia), Stockholm (Sweden) and Prague (Czech Republic). Dispersion models have been proven to provide reliable results on local to global scale in several studies and are essential tools of risk management. However, the users must not

ignore possible error sources in complex weather situations characterized by low-level inversions with fog and a significant directional wind shear.

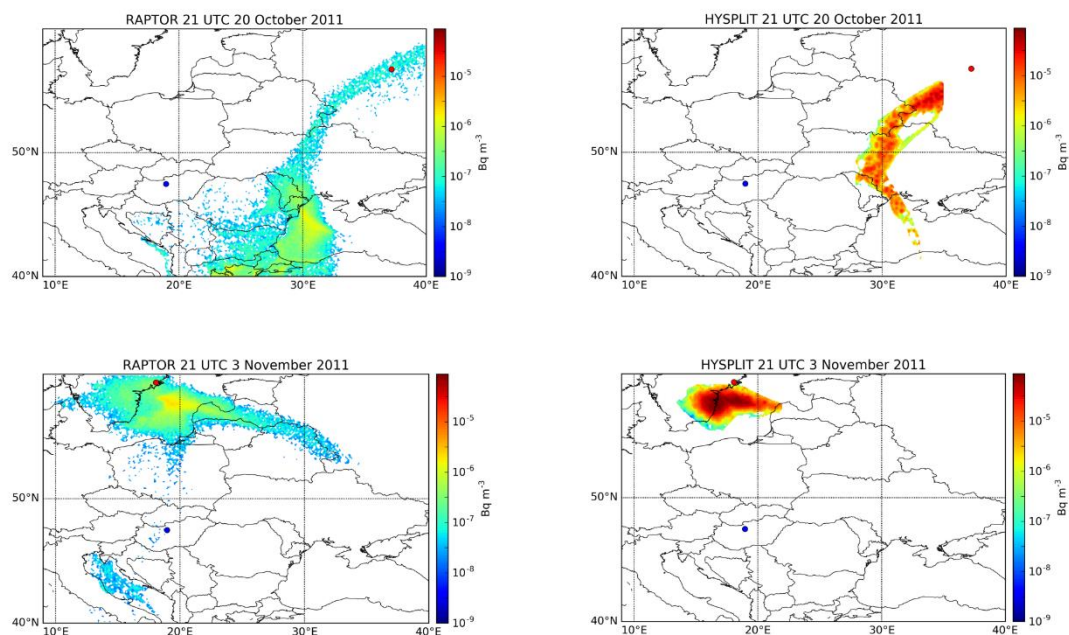


Figure 3.1 Modeled surface ^{131}I concentrations at 21 UTC, 20 October (top) and 3 November (bottom) 2011 with RAPTOR (left) and HYSPLIT (right) models, 84 hours after the beginning of emission from Budapest (blue dot). Detection sites of Dubna (top) and Stockholm (bottom) are marked with red dot.

In three of the four investigated cases, the existence and the arrival time of the plume above the detection sites was well predicted. However, concentration values showed large uncertainty and variability among the models. In cases of Dubna and Stockholm, the simulated pollutants were elevated to higher altitudes that lead to a significant underestimation of surface concentrations. Precipitation occurring near the two cities during the sampling period caused relatively high surface concentration values.

In case of the ^{131}I detection in Prague, 4 November 2011, the simulated plume of Lagrangian models did not or only marginally affect the city. On the other hand, the more detailed simulation of WRF-Chem showed the plume to largely move towards Prague. This contradiction was explained with a strong low-level wind shear and the overestimation of planetary boundary height in the GFS meteorological data. We propose that possible errors in model results can be identified without costly WRF-Chem simulations simply considering deterministic trajectory calculations and surface wind observations. The results underline the importance of the identification of low-level inversions and wind shears in the interpretation of dispersion model results.

4. Time-dependent downscaling of PM2.5 predictions from CAMS air quality models to urban monitoring sites in Budapest using a linear multi-model fusion method

Budapest, the capital of Hungary, has been facing serious air pollution episodes in the heating seasons similar to other metropolises. A dense urban air quality monitoring network is available; however, air quality prediction is still challenging. For this purpose, 24-hour PM2.5 forecasts obtained from 7 individual models of the Copernicus Atmosphere Monitoring Service were downscaled by using hourly measurements at 6 urban monitoring sites in Budapest for the heating season of 2018-2019. A 10-day long training period was applied to fit spatially consistent model weights to construct a linear combination of CAMS models for each day, and the 10-day additive bias was also corrected. Results were compared to the CAMS ensemble median, the 10-day bias-corrected CAMS ensemble median, and the 24-hour persistence. Downscaling reduced root mean square error (RMSE) by 1.4 $\mu\text{g}/\text{m}^3$ for the heating season and by 4.3 $\mu\text{g}/\text{m}^3$ for episodes compared to the CAMS ensemble, mainly by eliminating the general underestimation of PM2.5 peaks. As a side-effect, an overestimation was introduced in rapidly clearing conditions. Although the bias-corrected ensemble and model fusion had similar overall performance, the latter was more efficient in episodes. Downscaling of CAMS models was found to be capable and necessary to capture high wintertime PM2.5 concentrations for the short-range air quality prediction in Budapest.

Data fusion methods for downscaling air quality model results are widely used to improve spatial model accuracy by adjustment with point measurements, to provide locally optimized predictions at monitoring sites, and to generate measurement-adjusted boundary conditions for nested models. Single-model downscaling methods include the correction of systematic bias and the blending of model predictions with interpolated observational fields. Ensemble downscaling methods create an optimized combination of model outputs using spatially dependent, or spatially consistent weights. Recently, the methodology of data fusion has been extended to construct very fine-scale air quality fields by using data from low-cost sensors.

In this study, we applied a linear multi-model fusion method with time-dependent weights to downscale CAMS PM2.5 predictions to urban monitoring sites in Budapest in the heating season of 2018-2019.

Method

A fusion of CAMS air quality models was applied to downscale PM2.5 air quality predictions to monitoring sites in Budapest. The fused prediction $c_{fusion,x,t}$ for location x and time t was constructed as a time-dependent linear combination of the 7 independent models:

$$c_{fusion,x,t} = w_{0,t} + \sum_{i=1}^7 w_{i,t} c_{i,x,t}$$

The prediction $c_{i,x,t}$ was (a) the raw (b) the bias-corrected PM2.5 prediction from the i^{th} CAMS model for time t and the nearest grid point to monitoring location x . Model weights $w_{0-7,t}$ were optimized at each day by minimizing the regularized RMSE cost function J_t for all available locations over the training period of $[t - T - d: t - d]$.

$$J_t = \sqrt{\frac{1}{X \cdot T} \sum_{x=1}^X \sum_{\tau=t-T-d}^{t-d} (c_{fusion,x,\tau} - c_{obs,x,\tau})^2} + R$$

where X is the number of observation sites with available hourly data in the training period and T is the length of the training period. A delay d was introduced to simulate delays in the availability of monitoring data. Note that the model weights were time-dependent but spatially consistent, and all stations were included to optimize the model weights to enhance the consistency of the fused prediction for the entire urban area. To reduce overfitting, a regularization term R was added to the cost function containing two terms to regularize deviations from the ensemble mean and large temporal shifts in consecutive model weighting, respectively:

$$R = \alpha \sum_{i=1}^7 \left(w_{i,t} - \frac{1}{7} \right)^2 + \beta \sum_{i=1}^7 (w_{i,t} - w_{i,t-1})^2$$

Depending on the available urban monitoring sites reporting hourly PM2.5 concentrations in Budapest, $X = 4$, $X = 5$ or $X = 6$ was used (see data availability in Table 1). The training period was set to 10 days, i.e. $T=240$ was applied for hourly data. Thus, a total of 960–1440 observation-prediction pairs were used to fit 8 independent weights for each day, representing each CAMS model’s relevance for predicting urban PM2.5 concentrations during the past 10 days, plus a zero-degree term. Regularization strength parameters α and β were set to 0.1 and 100, respectively. The delay d in monitoring data availability was set to 24 hours permitting manual data quality assurance.

Hourly PM2.5 monitoring data were obtained from the Hungarian Air Quality Monitoring Network (<http://levegominoseg.hu>) for 6 sites in Budapest, including city and suburban locations. Near-real-time, daily initialized 24-hour regional model predictions were obtained from the Copernicus Atmosphere Monitoring Service (<https://atmosphere.copernicus.eu/>). The data fusion method was implemented in two ways: (a) using the raw CAMS forecasts as input predictions; (b) correcting the previous 10-day additive bias independently for each model and using the bias-corrected CAMS model forecasts as input predictions for the fusion.

Results

A linear model fusion with time-dependent but spatially consistent weights of CAMS air quality models was applied to obtain 24-hour PM_{2.5} measurements for Budapest. Figure 4.1 presents the observed time series, the fused prediction and the CAMS ensemble median for three urban sites. Time-dependent bias correction was also applied for each day by removing the additive bias of the previous 10-day long window for each day. The bias-corrected ensemble (BC_ENSEMBLE) and the fusion of bias-corrected individual models (BC_fusion) are also presented with points in Figure 4.1.

CAMS ensemble median generally underestimated urban PM_{2.5} concentrations, especially during episodes. Downscaled forecasts, both by time-dependent bias correction of the CAMS ensemble and the fusion of individual CAMS models, largely improved the predictions and could better capture the episode peaks (Figure 4.1). Exceptions were the clear-up days following episodes, overestimated by the downscaled predictions (e.g. 14-20 Nov, 23-30 Dec). If the 10-day training period included an episode, a large negative bias was corrected and/or the model predicting higher concentrations was overweighted, which brought overestimations after the episode. Meanwhile, the clear-up event was obviously captured by all models, and the overestimation was less severe in the data fusion model than for the bias-corrected CAMS ensemble. Accordingly, daily root mean square error (RMSE) calculated from hourly model-observation pairs at all available observation sites (Figure 3) was lower for the fused model than for any individual model during the entire heating season, except for the clear periods following an episode.

Observed intra-urban variability reached 20 µg/m³ difference between peak 24-hour PM_{2.5} concentrations among urban sites. As expected, this could not be captured by the models, and the fused model underestimated peaks in more polluted (Gergely utca), and overestimated peaks in less polluted (Kőrakás park) sites. (Figure 4.1) Site-specific weighting might solve this issue, but this research aimed to produce a downscaled model for the entire urban area, and not for specific local environments.

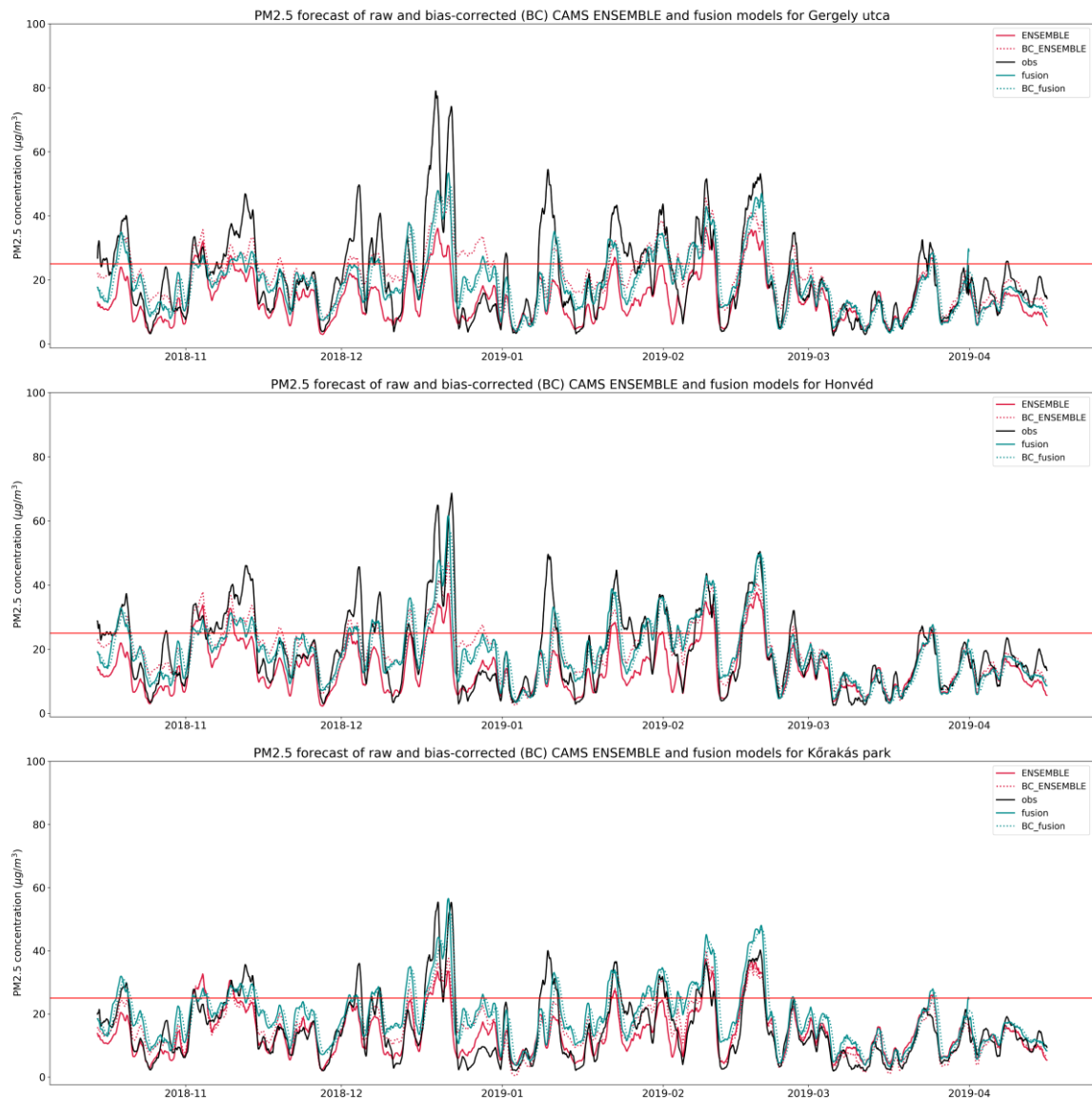


Figure 4.1. 24-hour moving average PM_{2.5} measurements (black) at three urban monitoring sites compared with the CAMS ensemble median (red) and the fused prediction (blue). Bias-corrected CAMS ensemble (BC_ENSEMBLE) and fusion of bias-corrected individual models (BC_fusion) are shown with points. The WHO guideline 25 µg/m³ is marked.

A downscaling method using 24-hour forecasts from 7 independent air quality models of the Copernicus Atmosphere Monitoring Service (CAMS) was introduced to improve PM_{2.5} predictions in Budapest in the heating season of 2018-2019. Hourly observations from 6 urban monitoring sites were used to fit time-dependent, but spatially consistent weights in a 10-day long moving training period to produce a model-weighted prediction. A 10-day additive bias was also corrected for each model and the CAMS ensemble median.

Both the bias-corrected ensemble and the model fusion improved model prediction compared to the original CAMS ensemble. The RMSE in the overall heating season improved from 11.4 µg/m³ to 10.0 µg/m³. The added value of downscaling was more pronounced during episodes, improving RMSE from 17.2 µg/m³ to 12.9 µg/m³. This came at the price of introducing forecast error in rapidly changing conditions due to the lagged training period, however, the time and direction of pollution changes were

still captured. The European Air Quality Index (EAQI) category was correctly predicted in 51% of the hourly cases. With downscaling, the same accuracy could be reached in episodes compared to the 32% of the original CAMS ensemble. While bias-corrected ensemble and model fusion had similar overall performance, the latter was more efficient to predict PM_{2.5} peaks and the time-dependent model weighting benefited from all the widely different CAMS model systems in their optimal conditions.

5. A review of numerical models to predict the atmospheric dispersion of radionuclides

The field of atmospheric dispersion modeling has evolved together with nuclear risk assessment and emergency response systems. Atmospheric concentration and deposition of radionuclides originating from an unintended release provide the basis of dose estimations and countermeasure strategies. To predict the atmospheric dispersion and deposition of radionuclides several numerical models are available coupled with numerical weather prediction (NWP) systems. This work provides a review of the main concepts and different approaches of atmospheric dispersion modeling. Key processes of the atmospheric transport of radionuclides are emission, advection, turbulent diffusion, dry and wet deposition, radioactive decay and other physical and chemical transformations. A wide range of modeling software are available to simulate these processes with different physical assumptions, numerical approaches and implementation. The most appropriate modeling tool for a specific purpose can be selected based on the spatial scale, the complexity of meteorology, land surface and physical and chemical transformations, also considering the available data and computational resource. For most regulatory and operational applications, offline coupled NWP-dispersion systems are used, either with a local scale Gaussian, or a regional to global scale Eulerian or Lagrangian approach. The dispersion model results show large sensitivity on the accuracy of the coupled NWP model, especially through the description of planetary boundary layer turbulence, deep convection and wet deposition. Improvement of dispersion predictions can be achieved by online coupling of mesoscale meteorology and atmospheric transport models. The 2011 Fukushima event was the first large-scale nuclear accident where real-time prognostic dispersion modeling provided decision support. Dozens of dispersion models with different approaches were used for prognostic and retrospective simulations of the Fukushima release. An unknown release rate proved to be the largest factor of uncertainty, underlining the importance of inverse modeling and data assimilation in future developments.

State-of-the-art numerical weather prediction systems coupled with atmospheric chemistry and transport models are powerful tools for the simulation of atmospheric dispersion, turbulent diffusion, wet and dry deposition and decay of radionuclides from accidental releases on local to global scale. Since the Chernobyl accident, dispersion models have evolved from standalone regulatory software to complex emergency response systems and multi-scale research frameworks. Rapidly developing NWPs and computational capacities allow more and more detailed dispersion simulations. Meanwhile, serious bottlenecks of model accuracy are still present. The main source of error is the uncertainty of the temporal evolution of the emission process, although the location of the source is usually well known. Mesoscale atmospheric phenomena (convection, inversion) and the uncertain wet deposition are also important sources of error.

On the local scale, recent developments point towards the more detailed description of planetary boundary layer turbulence with computationally intensive large eddy simulation (LES) models. However, the nesting of CFD software into regional scale dispersion models is still a challenging task. On regional

to global scale, ensemble weather predictions lead to a probabilistic approach of dispersion simulations. In the recent years, inverse modeling has got into the focus of research. Source-receptor sensitivity maps are produced to study transboundary air pollution and to reconstruct the spatial and temporal structure of the emission processes.

Among the rich variety of different approaches and implementations of atmospheric dispersion models, the most appropriate tool for a specific task can be selected based on the spatial scale, the complexity of processes (in terms of meteorology, orography, deposition, chemistry), the available data and computational resource as well as the output requirements. Fast response Gaussian models provide an efficient tool for emergency response and long-term impact studies on the local scale. From regional to global scale, Eulerian (e.g. CMAQ, WRF-Chem) and Lagrangian (e.g. HYSPLIT, FLEXPART) models are applied. Development, optimization and evaluation of dispersion models require validation datasets, many of which are related to radioactive releases. Online integrated meteorology-dispersion coupling, data assimilation and ensemble forecasting are computationally demanding tools that can significantly improve model accuracy.

6. Traffic originated urban air pollution estimation based on atmospheric-chemistry model

Traffic-related air pollution has become a serious issue in European cities. Budapest, the capital of Hungary and the 9th largest city of the EU, has been facing high concentrations of particulate matter (PM) and NO₂, which exceeding the guidelines defined by the European Environmental Agency. The World Health Organization estimated an approximate 8,000 deaths related to outdoor air pollution in Hungary each year. While most of the PM10 pollution is attributable to domestic heating and large-scale transport, NO₂ is a mainly traffic-related pollutant.

Prediction of the air quality for Budapest is performed by the Copernicus Atmospheric Monitoring Service and the Hungarian Meteorological Service. Emission inventories for these models are available on grids with 0.1° or 7 km horizontal resolution. However, these inventories cannot describe the fine spatial and diurnal variations of urban traffic. To estimate traffic emissions, top-down and bottom-up approaches are used. A top-down method uses observed air quality data on monitoring sites and an inverse atmospheric transport model to obtain an emission field without any actual data on the traffic characteristics. A bottom-up approach couples a traffic model with the atmospheric transport model and provides an emission inventory based on the macroscopic traffic characteristics.

Besides operational air quality prediction, coupled traffic and atmospheric modeling can be used to assess the impacts of emission reduction policies, for source attribution, to investigate future scenarios and to better understand the relationship between traffic characteristics and air quality. Coupling traffic and atmospheric models also enable the use of real-time GPS-based traffic data as an input for air quality nowcasting. Parallel usage of top-down and bottom-up methods helps to investigate the impact of vehicles with increased emission factor due to bad maintenance or a malicious bypass of emission reduction systems.

Dispersion model

Atmospheric dispersion of pollutants was simulated with the WRF-Chem online coupled atmospheric chemistry transport model adapted for the simulation of air quality in Hungary. WRF-Chem is one of the most widely used mesoscale model for weather and air quality prediction, and has been successfully coupled with traffic emission models in several applications.

Results

To evaluate the model in a case study, a period was selected when the impact of traffic-related emissions are assumed to be the strongest compared to other factors determining the air quality of Budapest (i.e., domestic heating, large-scale transport, weather). The heating season (October–April) was avoided to eliminate domestic sources, while weekends and the summer holiday season were also avoided because of the reduced commutation demand, not represented by the applied MTM model. Based on these criteria, 26–27 September 2016 was defined as the study period with calm anticyclonic weather and very weak winds that minimized the weather-related uncertainty and the impact of large-scale transport. It can be

reasonably assumed that in these conditions, traffic emissions were the main driver of the air quality of Budapest. This enables a qualitative comparison of obtained results with measurements, however, quantitative validation still remains impossible as non-traffic sources always persist. The selected period was also suitable to investigate the temporal and spatial pattern of concentrations caused by the coupled effect of commutation and NO_x - O_3 photochemistry, a typical air pollution scenario in summer anticyclones.

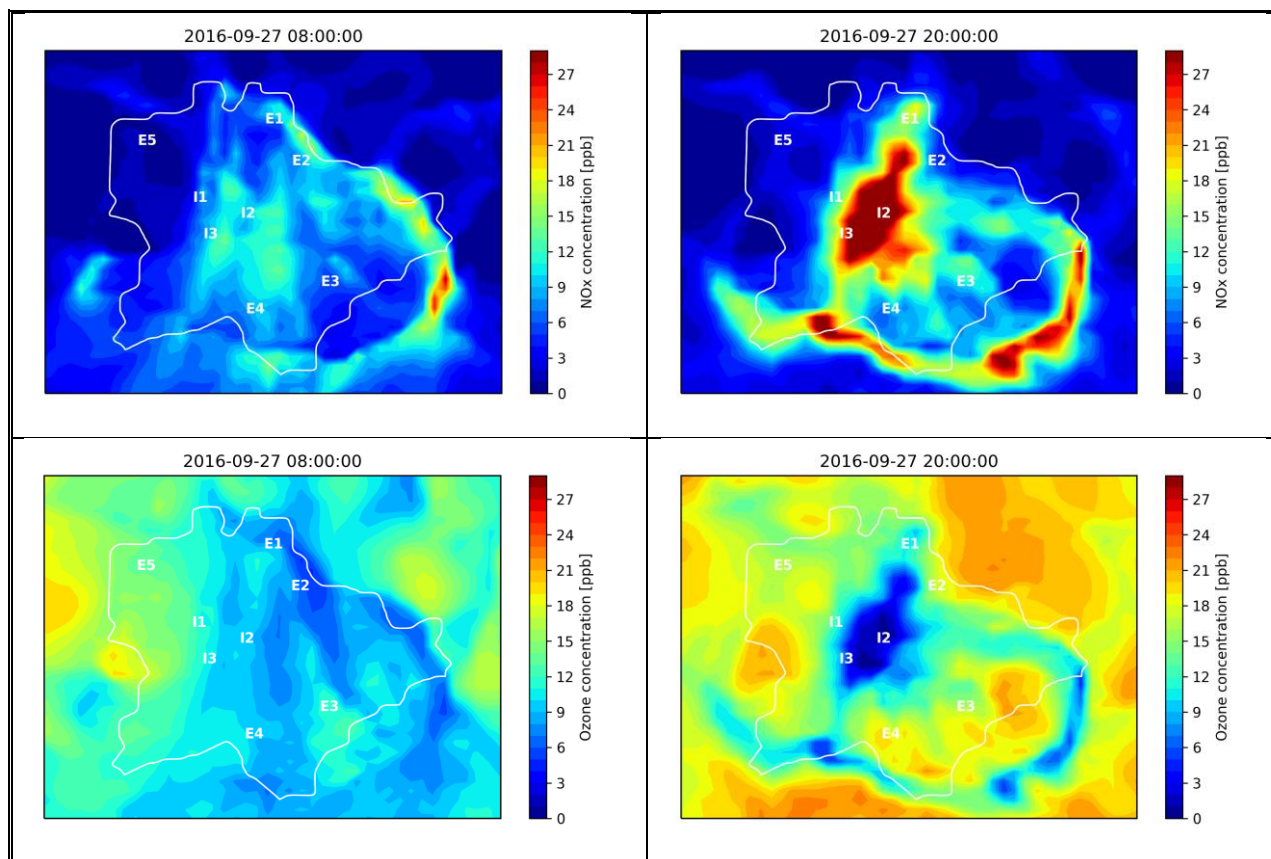


Figure 6.1 Simulated NO_x (upper row) and O_3 (lower) concentrations caused by traffic emission at 6 and 18 UTC (8 AM and 8 PM local time), 27 September 2016.

Figure 6.1 shows the simulated morning (8 AM local time) and evening (8 PM local time) concentrations of NO_x and secondary ozone. The spatial structure of the NO_x field follows closely the traffic density, however, calm wind allows the NO_x emission from several hours of high traffic during the afternoon to accumulate in the urban air. Therefore, evening concentrations were simulated to be higher than those in the morning rush hours, and the maximum NO_x concentrations were found in the late evening hours (8-11 PM local time).

Ozone concentrations show a clear daytime and afternoon maximum, while concentrations are low in the morning hours. The inverse relationship between NO_x and O_3 concentrations is well observable, explained by the fact that direct NO emission decays ozone. Highest ozone concentrations are found in the southern and eastern suburbs, and mainly in the agglomeration out of the city borders. However, the two areas are clearly divided by a significant feature of the urban structure, the M0 highway ring that largely reduces O_3 and increases NO_x pollution in a 1–2 km wide band.

In conclusion, a coupled simulation of traffic network, traffic emission, atmospheric transport and atmospheric photochemistry is presented in an urban case study, representing a typical weekday scenario in an early autumn anticyclone. The temporal and spatial pattern of traffic-related NO_x and O_3 air pollution is modeled and described with 1 km horizontal and 1 hour temporal resolution. The simulated diurnal trends are in good agreement with measurements, but NO_x concentrations are seriously underestimated. General underestimation (or decrease) of urban NO_x emission, due to either lower traffic density or emission factors, causes an overestimation (or increase) of ozone levels in the city center and at night, but it causes an underestimation (or decrease) of suburban ozone peaks. A uniform traffic emission reduction results in a nearly linear decrease of NO_x levels; a small decrease of CO levels in the city center and its downwind area; and a complex response of ozone levels with increasing daily mean levels, especially in the high-traffic areas, but decreasing downwind suburban ozone peaks.

7. Air quality modelling using dissipative particle dynamics (DPD)

Basic of the dissipative particle dynamics

The dynamics of the fluid flow, is usually simulated by the Navier-Stokes equations, which are mathematically partial differential equations with appropriate initial and boundary conditions. In the complex three-dimensional domain the application of boundary conditions can be a challenging task. Additionally, these calculations are computationally expensive and time consuming. We provide here some examples for simulating time dependent fluid flow using DPD (dissipative particle dynamics) method. DPD is a mesoscopic simulation method and lies between the macroscale and the microscale approaches. In macroscopic simulations the system is generally described by partial differential equations, however, in nanoscale and microscale the continuum approach is no longer valid and atomistic models should be used. For a mesoscale simulation the atomistic description is computationally too expensive. In order to decrease the number of the particles and increase the time step of the simulations some particles must be handled together (coarse graining). Increasing the size of the particles involves the change in the interaction potential between the grains. The repulsive force between two atoms increases rapidly with distance although with our new particles this force will be smoother which results in a greater time step and longer simulation time. Furthermore, when two strongly coarse grained particles collide a partially inflexible collision occurs. Particle has a lot of inner degree of freedom so the motion energy of the particle transforms into internal energy (inner particle motion). To achieve this inflexible collision new types of forces should be introduced - dissipative and random forces - which make the system dissipative, but conserve the mass and momentum. If the time integration is accurate (with an appropriate small time step) and the continuum concepts are valid (enough large system) then the DPD model conforms the Navier-Stokes equation.

Equation of motion

In a DPD simulation continuous space, and in the time integration, discrete time coordinates are used. We can describe the system with the Newton's second law:

$$\frac{d\mathbf{r}_i}{dt} = \mathbf{v}_i,$$
$$m_i \frac{d\mathbf{v}_i}{dt} = \mathbf{F}_i^{ext} + \mathbf{F}_i^{int},$$

where \mathbf{r}_i , \mathbf{v}_i , and m_i are the position, the velocity and the mass of the i th particle, \mathbf{F}_i^{ext} and \mathbf{F}_i^{int} are the sum of the external and internal forces.

Internal forces and pairwise interactions

One of the most time consuming parts of a particle-based simulation is the calculation of the pairwise interactions. Fortunately the methods developed in molecular dynamics can be used in DPD as well. The interacting particles, which distance is less than the cut-off distance r_c , can be identified using cell or

neighbour lists. The computational cost can be reduced from $O(N^2)$ to $O(N)$, where N is the number of particles in the system. The internal forces acting on the i th particle can be divided into three parts:

$$\begin{aligned}\mathbf{F}_i^{int} &= \sum_{i \neq j} (\mathbf{F}_i^C + \mathbf{F}_i^D + \mathbf{F}_i^R), \\ \mathbf{F}_i^C &= a_{ij} \omega^C(r_{ij}) \mathbf{e}_{ij}, \\ \mathbf{F}_i^D &= -\gamma \omega^D(r_{ij}) (\mathbf{e}_{ij} \mathbf{v}_{ij}) \mathbf{e}_{ij}, \\ \mathbf{F}_i^R &= \sigma \omega^R(r_{ij}) \theta_{ij} \mathbf{e}_{ij},\end{aligned}$$

where \mathbf{F}_i^C , \mathbf{F}_i^D and \mathbf{F}_i^R are the conservative, the dissipative and the random forces acting on the i th particle due to the j th particle interaction. $\mathbf{r}_{ij} = \mathbf{r}_i - \mathbf{r}_j$ and $\mathbf{e}_{ij} = \mathbf{r}_{ij}/|\mathbf{r}_{ij}|$ are the vector and the unit vector from j th particle to i th and $\mathbf{v}_{ij} = \mathbf{v}_i - \mathbf{v}_j$, a_{ij} , γ , σ are constants reflecting the strength of the interactions. With this parameters it is possible to fine tune the phenomenological properties of the system such as the surface tension, compressibility, diffusivity or viscosity. ω^D and ω^R are the weight functions, which depend only on the distance of the particles ($r_{ij} = |\mathbf{r}_{ij}|$). θ_{ij} is a Gaussian white noise ($\theta_{ij} = \theta_{ji}$).

The pairwise interactions $\mathbf{F}_{ij} = -\mathbf{F}_{ji}$ act in the line of the particle centers, and they ensure the linear and angular momentum conservation. The dissipative and the random forces do not appear in a classical molecular dynamics (MD) simulation. The dissipative force slows down the particles, and it represents the viscosity. Without the random force the particles would freeze, and it represents the thermal fluctuations. The ratio of these two forces adjusts the temperature of the system T , and it acts like a built-in thermostat. According to the fluctuation-dissipation theorem²³

$$\begin{aligned}\omega^D(r_{ij}) &= [\omega^R(r_{ij})]^2, \\ \gamma &= \frac{\sigma}{2k_B T}.\end{aligned}$$

The random force in incremental form can be expressed as

$$\mathbf{F}_{ij}^R = \sigma \omega^R(r_{ij}) \zeta_{ij} \mathbf{e}_{ij} \sqrt{\Delta t},$$

where ζ_{ij} is a random variable with zero mean and unit variance, $\zeta_{ij} = \zeta_{ji}$, and ζ_{ij} is independent in every time step and for each pair of particles.

Weight functions

In DPD the weight functions are smooth compared to the atomistic description due to the highly coarse grained particles. The soft interactions make it possible to use greater time steps. A commonly used form of the weight functions is the following

$$\omega^D(r_{ij}) = [\omega^R(r_{ij})]^2 = \begin{cases} (1 - r_{ij}/r_c)^5 & \text{if } r_{ij} < r_c \\ 0 & \text{if } r_{ij} \geq r_c \end{cases},$$

$$\omega^C(r_{ij}) = \begin{cases} (1 - r_{ij}/r_c) & \text{if } r_{ij} < r_c \\ 0 & \text{if } r_{ij} \geq r_c \end{cases},$$

where $\omega^D(r_{ij})$, $\omega^R(r_{ij})$ and $\omega^C(r_{ij})$ are the weight functions for the dissipative, random and conservative interactions. Above the cut-off distance (r_c) the interactions are considered to be negligible, which reduces the number of the interacting particle pairs. s has a strong effect on the dynamic behavior of the system. It influences the viscosity of the medium and the diffusivity of particles. A general choice is $s = 2.0$.

Fluid simulation

Using the above conservative weight functions there are no attractive interactions in the system and a condensed phase cannot form. In order to simulate liquids, keeping the beneficial properties of the DPD simulations, we have to introduce some soft long-range attractive component into the conservative weight function. It is possible to construct short-range repulsive and long-range attractive soft potentials with polynomial functions using the following forms

$$U^C(r_{ij}) = a_{ij} \left(AW^R(r_{ij}, r_c^R) - BW^A(r_{ij}, r_c^A) \right),$$

$$W(r_{ij}, r_c) = \begin{cases} 1 - \frac{3}{2} \left(\frac{2r_{ij}}{r_c} \right)^2 + \frac{3}{4} \left(\frac{2r_{ij}}{r_c} \right)^3 & \text{if } 0 \leq \frac{2r_{ij}}{r_c} < 1 \\ \frac{1}{4} \left(2 - \frac{2r_{ij}}{r_c} \right)^3 & \text{if } 1 \leq \frac{2r_{ij}}{r_c} < 2, \\ 0 & \text{if } \frac{2r_{ij}}{r_c} \geq 2 \end{cases},$$

where $W(r_{ij}, r_c)$ is a cubic spline, which depends on the particle-particle distance and the cut-off radius. Here the conservative potential function U^C has two different cut-off radii: r_c^R is for the short-range repulsive and r_c^A is for the long-range attractive interaction. a_{ij} , A and B are non-negative constants. The conservative force acting on the i th particle (due to the interaction with the j th particle) can be calculated from the potential gradient

$$\mathbf{F}_{ij}^C = -\nabla U^C(r_{ij}).$$

External forces and time integration

In a particle-based simulation it is easy to handle external forces. We can compute the effect of an external field (in our case the gravitational field) in the following form

$$\mathbf{F}_i^{ext} = m_i \mathbf{g},$$

where \mathbf{F}_i^{ext} is the sum of the external forces on the i th particle. Here we used just a gravitational field, and \mathbf{g} and m_i are the gravity acceleration and the mass of the i th particle, respectively.

Time integration is a crucial part of the particle-based simulations. In DPD simulations Groot and Warren offered a modified velocity-Verlet algorithm, which is a predictor-corrector method. At the beginning of a time step a predicted velocity ($\hat{\mathbf{v}}$) is calculated with an empirical constant λ , and once forces are calculated the corrected velocities are calculated as follows

$$\begin{aligned}\mathbf{r}_i(t + \Delta t) &= \mathbf{r}_i(t) + \Delta t \mathbf{v}_i + \Delta t^2 \mathbf{f}_i(t), \\ \hat{\mathbf{v}}_i(t + \Delta t) &= \mathbf{v}_i(t) + \lambda \Delta t \mathbf{f}_i, \\ \mathbf{f}_i(t + \Delta t) &= \mathbf{f}_i(\mathbf{r}_i(t + \Delta t), \hat{\mathbf{v}}_i(t + \Delta t)), \\ \mathbf{v}_i(t + \Delta t) &= \mathbf{v}_i(t) + 0.5 \Delta t (\mathbf{f}_i(t) + \mathbf{f}_i(t + \Delta t)),\end{aligned}$$

where $\mathbf{f}_i(t) = \mathbf{F}_i(t)/\mathbf{m}_i$, $\mathbf{r}_i(t)$, $\mathbf{v}_i(t)$ and $\mathbf{r}_i(t + \Delta t)$, $\mathbf{v}_i(t + \Delta t)$ are old and the new position and velocity of the i th particle.

Boundary conditions

At the boundary of the simulation domain it is possible to use *immobile particles*, which can act as a wall in the system. However, particles can penetrate into the wall because of the applied smooth repulsive interactions. In some cases - for example if we would like to build up a semipermeable obstacle or membrane - this penetration can be advantageous, but we have to prevent it at the boundary of a solid wall. One possibility is to make the wall impenetrable by putting frozen particles into the wall in a higher density or using stronger repulsive forces among the wall particles. It should be noted that this approach can lead to density oscillations.

Another possibility to prevent the penetration of the particles into the wall is to apply reflection of the particles at the boundary. In *free-slip* conditions the normal vector of the particles are reflected in the boundary and in *no-slip* condition all velocity components are reversed.

Results

To illustrate the magnificent power of the DPD simulations, we calculated the structure of the fluid flow in a street canyon (Figure 7.1). The results obtained using this strategy is consistent with the results using Navier–Stokes equations. DPD simulations can be performed easily in a complex cases such as fluid flow around obstacles and inside them. There is an increased demand in the air quality modelling at local scales that how the trees and bushes affects the fluid flow around and inside them. It is evident that the trees/bushes are (semi)permeable to the fluid and air pollutants, using the DPD it is easy to generate objects having weaker or stronger interactions between their particles. Weaker interactions generate objects with more permeability for the fluid flow and air pollutants. Mathematically, using Navier–Stokes equations it is almost impossible or require

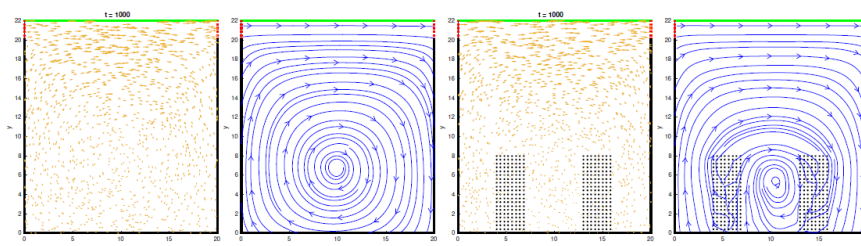


Figure 7.1 Street canyon simulations based on DPD.

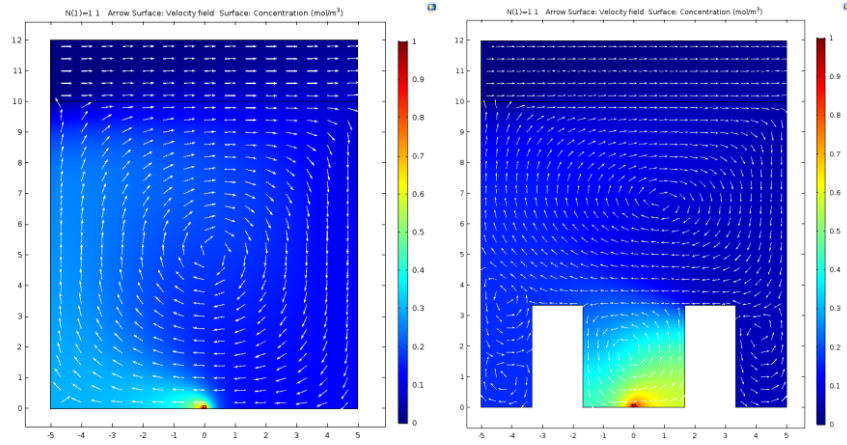


Figure 7.2 Street canyon simulations based on Navier–Stokes equations.

In conclusion, we developed a new approach to simulate the fluid flow in the atmosphere. To illustrate our concept, we simulated fluid flows and concentration distribution of air pollutants in a street canyon with and without obstacles.

References

1. R Mészáros, Á Leelőssy, T Kovács, I Lagzi, Predictability of the dispersion of Fukushima-derived radionuclides and their homogenization in the atmosphere, *Scientific Reports* 6, 19915.
2. A Kovács, Á Leelőssy, R Mészáros, I Lagzi, Online coupled modeling of weather and air quality of Budapest using the WRF-Chem model, *Időjárás* 123 (2), 203–215.
3. Á Leelőssy, R Mészáros, A Kovács, I Lagzi, T Kovács, Numerical simulations of atmospheric dispersion of iodine-131 by different models, *PLOS One* 12 (2), e0172312.
4. A Varga-Balogh, Á Leelőssy, I Lagzi, R Mészáros, Time-Dependent Downscaling of PM_{2.5} Predictions from CAMS Air Quality Models to Urban Monitoring Sites in Budapest, *Atmosphere* 11 (6), 669.
5. Á Leelőssy, I Lagzi, A Kovács, R Mészáros, A review of numerical models to predict the atmospheric dispersion of radionuclides, *Journal of Environmental Radioactivity* 182, 20–33.